Relativistic *ab initio* interpretation of *L-K* vacancy sharing in ion–solid-target collisions

P. Kürpick, T. Baştuğ, W.-D. Sepp, and B. Fricke
Fachbereich Physik, Universität Kassel, 34109 Kassel, Germany
(Received 15 March 1995)

The first experiments measuring the impact-parameter-dependent *L-K* vacancy sharing in ion–solid-target collisions started almost two decades ago. A rather qualitative explanation of the vacancy sharing process was achieved in the framework of the $2p\pi$-$2p\sigma$ coupling scheme developed by Briggs and Taulbjerg, but for most of the collision systems significant discrepancies remained. Even a multiple collision calculation using the $2p\pi$-$2p\sigma$ coupling scheme, as undertaken by Schuch *et al.*, did not improve the agreement with the experimental results and left a lack of an explanation, calling for first-principles calculations. Using our *ab initio* relativistic Dirac-Fock-Slater many-electron basis set method, we confirm that both a qualitative and quantitative explanation can be given for the *L-K* vacancy sharing process in heavy ion–solid-target collisions. As an example, we compare our results with measurements for 108-MeV Br on Ni-solid targets.

PACS number(s): 34.50.−s, 31.15.Ar

I. INTRODUCTION

Over the last two decades a whole series of experimental studies on ion–solid-target collisions has been performed [1–11]. The main emphasis of the experimental workers has been to go beyond ion–gas-target systems and elucidate the complex mechanism of vacancy creation in outer shells and their further transfer to inner shells while the projectile passes the solid target.

Most of these measurements were interpreted in the $2p\pi$-$2p\sigma$ coupling scheme originally proposed by Fano and Lichten [12] and Taulbjerg and Briggs [13]. This rather simple model reduces the *L-K* vacancy transfer to the solely rotational coupling between the two molecular states $2p\pi$ and $2p\sigma$. It therefore neglects all other channels and especially the radial coupling and reveals a strong discrepancy from the experimental results for heavy ion–solid-target collision systems. For some lighter ion–solid-target collision system the $2p\pi$-$2p\sigma$ coupling scheme seems to give a qualitative explanation in the large impact parameter range but it fails to reproduce experimental $P(b)$ curves in the low impact parameter range [7]. Generally the maximum calculated with the scaling law of Briggs, Taulbjerg, and Vaaben [13] is shifted towards larger impact parameters. Attempts have been undertaken to interpret the measurements in terms of two-collision probabilities by folding Monte Carlo trajectory calculations for the projectile scattering with $2p\pi$-$2p\sigma$ vacancy sharing probabilities but they did not improve the agreement with experimental results, therefore leaving a lack of an explanation [7].

In this paper we show that these ion–solid-target measurements can be explained in the framework of a many-electron time dependent Dirac-Fock-Slater approach. Performing large-scale close coupling calculations with both relativistic Dirac-Fock-Slater eigenvalues and *ab initio* dynamic coupling matrix elements we get very good qualitative and quantitative agreement with experimental results, showing that a two-collision procedure is not needed. As an example, we focus on the system 108 MeV Br on Ni.

II. THEORY

Our relativistic Dirac-Fock-Slater linear combination of atomic orbitals–molecular orbital (LCAO-MO) basis set method has been presented in a series of former papers [14–17]. We therefore only give a short review. In order to solve the time dependent single-particle Dirac-Fock-Slater equation for the electronic part of the collision system

$$\left(\hat{t}+\hat{V}^N(t)+\hat{V}^C(t)+\hat{V}_\alpha^{Ex}(t)-i\hbar\frac{\partial}{\partial t}\right)\psi_i(t)=0, \qquad i=1,\ldots,N \quad (1)$$

we use an expansion of the wave function $\psi_i(t)$ into single-particle molecular functions $\phi_j(\vec{r};\vec{R}(t))$,

$$\psi_i(\vec{r},t)=\sum_j^M a_{ij}(t)\phi_j(\vec{r};\vec{R}(t)), \quad (2)$$

which themselves are linear combinations of atomic orbitals

$$\phi_j(\vec{r};\vec{R(t)})=\sum_{\nu=1}^S c_{j\nu}(\vec{R(t)})\xi_\nu(\vec{r};\vec{R}). \quad (3)$$

The atomic orbitals are numerically given four-component Dirac spinors and eigenfunctions of the atomic Dirac-Fock-Slater equation.

Inserting this ansatz (2) into Eq. (1) we get the well-known close coupling equations

$$\dot{a}_{ij} = \sum_m -a_{im}\langle\phi_j \mid \frac{\partial}{\partial t} \mid \phi_m\rangle \times \exp\left(-\frac{i}{\hbar}\int(\varepsilon_m - \varepsilon_j)dt'\right) \quad (4)$$

for the time dependent single-particle amplitudes a_{ij}. The close coupling equations (4) are solved for the N initial conditions

$$\lim_{t\to-\infty}\left(\psi_i(t) - \psi_i^0(t)\right) = 0, \quad i = 1, \ldots, N.$$

$\psi_i^0(t)$ is the initially occupied atomic orbital from which the molecular orbital $\psi_i(t)$ evolves.

The technical details on the generation of the molecular four-component basis functions by solving the secular equation

$$\mathbf{h}^{\mathrm{MO}}\mathbf{c} = \varepsilon\mathbf{S}\mathbf{c} \quad (5)$$

and calculation of the two types of *ab initio* dynamic coupling matrix elements,

$$\langle\phi_l \mid \frac{\partial}{\partial t} \mid \phi_m\rangle = \dot{R}\langle\phi_l \mid \frac{\partial}{\partial R} \mid \phi_m\rangle - \frac{i\dot{\theta}}{\hbar}\langle\phi_l \mid j_y^{\mathrm{CM}} \mid \phi_m\rangle,$$

the radial and rotational coupling, can be found in two earlier papers [14,17] and references therein. In Eq. (5) $\mathbf{h}^{\mathrm{MO}}$ means the Fock matrix, $\mathbf{c}$ the coefficient matrix, $\mathbf{S}$ the overlap matrix, and ε the diagonal eigenvalue matrix.

III. RESULTS AND DISCUSSION

Our relativistic *ab initio* method was already applied to a whole series of ion–gas-target collision systems as for example F-Ne [15] or S-Ar [16]. For all these systems we got both very good qualitative and quantitative agreement with measurement of the K-K vacancy sharing and the K-L charge transfer probability.

We recently started to study ion–solid-target systems

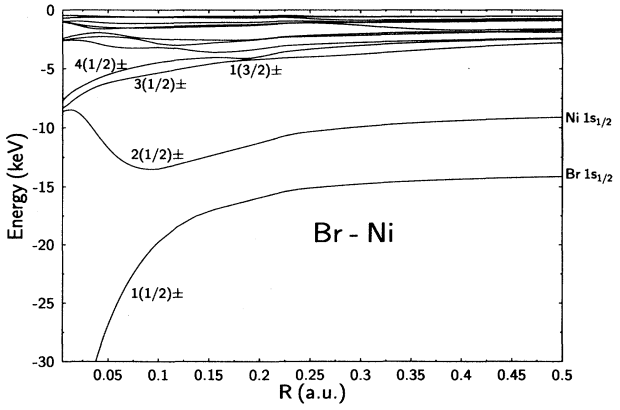

FIG. 1. Correlation diagram for the system Br-Ni.

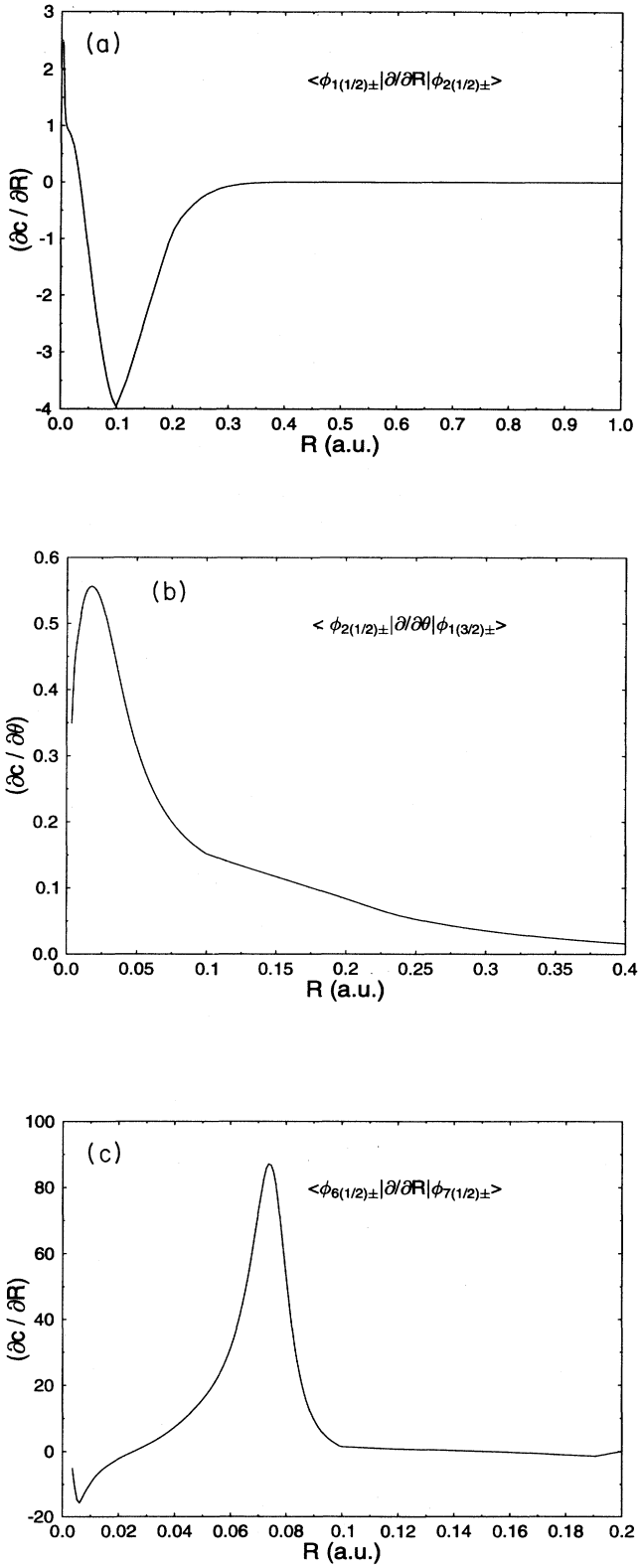

FIG. 2. (a) Radial coupling matrix element between the molecular $1(1/2)\pm$ and $2(1/2)\pm$ states. (b) Rotational coupling between the molecular $1(3/2)\pm$ and $2(1/2)\pm$ states. (c) Radial coupling matrix element between the molecular $6(1/2)\pm$ and $7(1/2)\pm$ states.

[17] where a whole series of experimental papers was published, most of them presuming the existence of *solid-target effects* [10] which should be responsible for the discrepancy between the $2p\pi$-$2p\sigma$ rotational coupling model and measurements for the impact-parameter-dependent K-vacancy probability.

In this paper we take up the system 108 MeV Br on a Ni-solid target. Detailed experimental results on the sum of projectile and target K-vacancy probabilities as a function of impact parameter b are given in the paper by Schuch *et al.* [7]. The experimental results, which are presented in Fig. 3 as black diamonds, show an oscillatory structure with an 11% maximum at about 1000 fm.

To set up the molecular basis functions a minimal atomic basis set was used which was built up by Br $1s_{1/2}$ to $3p_{3/2}$ and Ni $1s_{1/2}$ to a $4s_{1/2}$ atomic four-component wave function, thus leading to 48 molecular wave functions. Figure 1 shows the resulting correlation diagram for Br-Ni in the range of 0 to 0.5 a.u., where the secular equation (5) was solved for 80 internuclear distances. As an example of the 1128 *ab initio* dynamic coupling matrix elements which are used in the calculation, we present the three most dominant ones in Figs. 2(a)–2(c). These are the radial coupling matrix element between the molecular $1(1/2)\pm$ and $2(1/2)\pm$ states, which is the dominant matrix element for K-K vacancy sharing, the rotational coupling matrix element between $2(1/2)\pm$ and $1(3/2)\pm$ states, which is mainly reponsible for the K-L vacancy sharing, and the radial coupling matrix elements between the $6(1/2)\pm$ and $7(1/2)\pm$ states as an example of coupling between initial Ni $n = 2$ states. Each matrix element is shown in the R range where the main coupling between the corresponding states takes place. In the notation for the relativistic molecular levels, 1/2 and 3/2 denote the m_j quantum number.

As Schuch *et al.* [7] do not provide the initial charge states of the experimentally used Br projectile, we assume the Br-3d electrons and half of the 3s and 3p electrons to be ionized while the ion travels through the target, therefore dealing with a Br^{20+} projectile. For 108 MeV projectile energy this assumption is well justified as the M-shell electrons do not behave adiabatically at this impact energy. Furthermore, as Annett [4] showed in projectile charge resolved measurements of Cu on Ni, the actual charge state of the projectile in the solid can be widespread and quite different from its initially prepared charge state.

To calculate the summed $P_K(b)$ vacancy probability we follow a two-step procedure: In a first step we start from close coupling calculations with impact parameters between 0.1 and 1.0 a.u. and calculate the mean number of electrons transferred from the initially filled Br L shell to the vacant Br M shell. These large-scale close coupling calculations take all K and L electrons of Br and Ni into account and allow them to couple both with each other and with the empty M shell. Table I presents the asymptotic ($t = +\infty$) single-particle probabilities for the molecular $3(1/2)\pm$, $4(1/2)\pm$, $5(1/2)\pm$, and $1(3/2)\pm$ levels. One notices the strong promotion of electrons to higher shells, which leads to a mean probability of about 0.5 of having vacancies in each of the $3(1/2)\pm$, $4(1/2)\pm$, $5(1/2)\pm$, and $1(3/2)\pm$ levels.

In a second step we use these former mean vacancy probabilities for each of the molecular $3(1/2)\pm$, $4(1/2)\pm$, $5(1/2)\pm$, and $1(3/2)\pm$ levels, which in the incoming channel form the Br L shells. From calculations in the impact parameter range $0 \leq b \leq 0.1$ a.u. we then get the summed P_K vacancy probability in the Br-K and Ni-K shells. This summed P_K vacancy probability is shown in Fig. 3 as a full curve. Additionally we show the partial contributions of the molecular $3(1/2)\pm$, $4(1/2)\pm$, and $1(3/2)\pm$ vacancies. The contribution of the $5(1/2)\pm$ vacancies to the summed Br-K and Ni-K shell vacancy probability is quite small and therefore is not shown [18].

The experimentalists also tried to explain the experimental results in terms of both the $2p\pi$-$2p\sigma$ coupling and two-collision $2p\pi$-$2p\sigma$ coupling calculations. The later calculations were done by first evaluating a mean L-vacancy production probability and then utilizing the formalism of Anholt [19] to fold the L-vacancy production and the $2p\pi$-$2p\sigma$ rotational coupling probability for all combinations of scattering angles of two-collision events, which give the same detection angle θ relative to the beam axis [7]. Both of these calculated probabilities differ

TABLE I. Asymptotic single-particle probabilities for the occupation of the molecular levels $3(1/2)\pm$, $4(1/2)\pm$, $5(1/2)\pm$, and $1(3/2)\pm$.

	Single-particle probabilities ($t = +\infty$)			
b (a.u.)	$3(1/2)\pm$	$4(1/2)\pm$	$5(1/2)\pm$	$1(3/2)\pm$
0.100	0.346	0.428	0.401	0.609
0.200	0.384	0.348	0.422	0.545
0.400	0.578	0.344	0.479	0.649
0.600	0.340	0.653	0.832	0.805
0.800	0.320	0.558	0.895	0.943
1.000	0.692	0.334	0.962	0.989

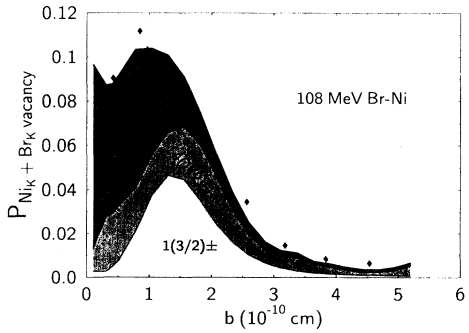

FIG. 3. Summed P_K vacancy: the experimental results from Schuch *et al.* [7] are shown as black diamonds. The partial contributions of the $3(1/2)\pm$, $4(1/2)\pm$, and $1(3/2)\pm$ vacancies are shown as differently shaded arrays. The total summed P_K vacancy probability is shown as a full line. The result obtained within the $2p\pi$-$2p\sigma$ coupling [7] scheme is shown as dotted curve.

only slightly from each other and fail to interpret the low impact parameter part of the experimental $P(b)$ curve. The two-collision $2p\pi$-$2p\sigma$ coupling calculation is shown in Fig. 3 as the dotted curve.

In the framework of our *ab initio* method the discrepancy between the results obtained within the $2p\pi$-$2p\sigma$ coupling scheme and the experimental $P(b)$ curve in the low impact parameter range as presented by Schuch *et al.* is now clear: the nonrelativistic $2p\pi$-$2p\sigma$ coupling would in our relativistic molecular picture correspond to the sole contribution of the $1(3/2)\pm$ vacancies which also tends to zero in the low impact parameter range.

IV. CONCLUSION

We presented large scale time dependent relativistic Dirac-Fock-Slater calculations on the impact parameter dependent charge transfer in collisions of 108 MeV Br on Ni-solid targets. The very good agreement with experimental results from Schuch *et al.* was achieved by taking the many-electron aspect of the collision system into account. It shows that at least for this collision system there is no need to suppose a multiple collision process to explain the experimental results.

ACKNOWLEDGMENTS

Support from the Deutsche Forschungsgemeinschaft for P.K. and T.B. is gratefully acknowledged. We further acknowledge the CPU time on the Siemens S400-Hessischer Höchstleistungsrechner at the Technische Hochschule in Darmstadt.

[1] G. Guillaume, P. Fintz, F. C. Jundt, K. W. Jones, and B. M. Johnson, Phys. Lett. A **68**, 39 (1978).
[2] I. Tserruya, H. Schmidt-Böcking, and R. Schuch, Phys. Rev. A **18**, 2482 (1978).
[3] B. M. Johnson, K. W. Jones, W. Brandt, F. C. Jundt, G. Guillaume, and T. H. Kruse, Phys. Rev. A **19**, 81 (1979).
[4] C. H. Annett, B. Curnutte, and C. L. Cocke, Phys. Rev. A **19**, 1038 (1979).
[5] R. Schuch, G. Nolte, B. M. Johnson, and K. W. Jones, Z. Phys. D **293**, 91 (1979).
[6] R. Schuch, G. Nolte, and H. Schmidt-Böcking, Phys. Rev. A **22**, 1447 (1980).
[7] R. Schuch, R. Hoffmann, K. Müller, E. Pflanz, H. Schmidt-Böcking, and H. J. Specht, Z. Phys. A **316**, 5 (1984).
[8] T. Kambara, T. Mizogawa, Y. Awaya, Y. Kanai, R. Schuch, K. Shima, and D. Trautmann, J. Phys. Soc. Jpn. **58**, 3929 (1989).
[9] G. Wintermeyer, V. Dangendorf, H. Schmidt-Böcking, T. Kambara, P. H. Mokler, R. Schuch, and I. Tserruya, Z. Phys. D **17**, 145 (1990).
[10] T. Kambara, R. Schuch, Y. Awaya, T. Mizogawa, H. Kumagai, Y. Kanai, H. Shibata, and K. Shima, Z. Phys. D **22**, 451 (1992).
[11] M. Jäger, M. Schulz, T. Kandler, A. Warczak, H. Bräuning, A. Demian, M. Damrau, A. El-Sadek, K. Freitag, J. Ullrich, and H. Schmidt-Böcking, Nucl. Instrum. Methods B (to be published).
[12] U. Fano and W. Lichten, Phys. Rev. Lett. **14**, 627 (1965).
[13] K. Taulbjerg and J. S. Briggs, J. Phys. B **8**, 1895 (1975).
[14] W.-D. Sepp, D. Kolb, W. Sengler, H. Hartung, and B. Fricke, Phys. Rev. A **33**, 3679 (1986).
[15] B. Thies, W.-D. Sepp, and B. Fricke, Phys. Lett. A **139**, 161 (1989).
[16] P. Kürpick, B. Thies, W.-D. Sepp, and B. Fricke, J. Phys. B **24**, L139 (1991).
[17] P. Kürpick, W.-D. Sepp, and B. Fricke, Phys. Rev. A **51**, 3693 (1995).
[18] P. Kürpick, H. J. Lüdde, W.-D. Sepp, and B. Fricke, Nucl. Instrum. Methods **94**, 183 (1994).
[19] R. Anholt, Nucl. Instrum. Methods **198**, 567 (1982).

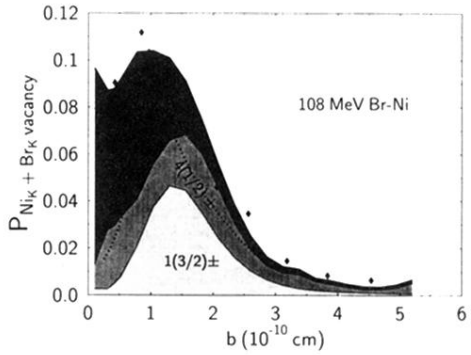

FIG. 3. Summed P_K vacancy: the experimental results from Schuch *et al.* [7] are shown as black diamonds. The partial contributions of the $3(1/2)\pm$, $4(1/2)\pm$, and $1(3/2)\pm$ vacancies are shown as differently shaded arrays. The total summed P_K vacancy probability is shown as a full line. The result obtained within the $2p\pi$-$2p\sigma$ coupling [7] scheme is shown as dotted curve.